

Confinement-induced zero-bias peaks in conventional superconductor hybrids

Jorge Cayao^{1,2} and Pablo Buset³

¹*Department of Physics and Astronomy, Uppsala University, Box 516, S-751 20 Uppsala, Sweden*

²*Theoretische Physik, Universität Duisburg-Essen and CENIDE, D-47048 Duisburg, Germany*

³*Department of Theoretical Condensed Matter Physics, Condensed Matter Physics Center (IFIMAC) and Instituto Nicolás Cabrera, Universidad Autónoma de Madrid, 28049 Madrid, Spain*

(Received 28 May 2021; revised 26 September 2021; accepted 27 September 2021; published 7 October 2021)

Majorana bound states in topological superconductors have been predicted to appear in the form of zero-bias conductance peaks of height $2e^2/h$, which represents one of the most studied signatures so far. Here, we show that quasi-zero-energy states, similar to Majorana bound states, can naturally form in any superconducting hybrid junction due to confinement effects, in the absence of spin fields and, thus, without relation to topology. Remarkably, these topologically trivial quasi-zero-energy states produce zero-bias conductance peaks, that could be similar to Majorana signatures, but develop a different peak height ($4e^2/h$) and are less stable under gating or depletion of the confined region. Our results put forward confinement as an alternative mechanism to explain the ubiquitous presence of trivial zero-bias peaks and quasi-zero-energy states in superconductor hybrids.

DOI: [10.1103/PhysRevB.104.134507](https://doi.org/10.1103/PhysRevB.104.134507)

I. INTRODUCTION

The realization of topological superconductivity featuring Majorana bound states (MBSs) in superconducting hybrid systems has lately been the subject of intense research due to its potential for technological applications [1–8]. The most promising approach involves semiconductor nanowires with strong spin-orbit coupling and proximity-induced conventional superconductivity [9,10]. Here, an external magnetic field drives such systems into a topological phase where MBSs emerge at zero energy and localize at each end of the wire. These properties enable MBSs to form the basis for qubit proposals robust against local perturbations [11–16], highlighting the importance of topological superconductivity in condensed matter physics.

The detection of MBSs has been mainly pursued by exploiting their zero-energy nature. Indeed, tunneling from a normal metal into a MBS has been predicted to result in a zero-bias conductance peak (ZBCP) of height $2e^2/h$ [17–22]. Subsequently, many experiments reported ZBCPs and interpreted them as strong evidence of MBSs [23–31]. Despite the significant experimental progress, the Majorana origin of ZBCPs has been recently questioned; in great part because several works have reported ZBCPs due to quasi-zero-energy states (qZESs) at finite magnetic fields but well below the topological phase and, hence, not tied to topology [32–54]. In this regard, recent theoretical efforts have suggested interesting detection protocols of MBSs [55–74], but the emergence of trivial qZESs still seems puzzling in conductance measurements.

Given the complex experimental setups involved in all Majorana platforms, it is fair to say that it still remains unclear if the emergence of trivial qZESs, and associated ZBCPs, is due to the interplay between superconductivity and magnetism,

the intrinsic inhomogeneities of superconducting heterostructures, or both. Understanding the mechanisms behind these nontopological states can help to interpret ZBCPs in experiments, rule out a possible Majorana origin, and envisage routes for mitigating the emergence of the unwanted qZESs.

In this work we demonstrate that qZESs can naturally emerge in hybrid junctions with conventional *s*-wave superconductors just due to confinement, and thus requiring neither magnetism nor spin-orbit coupling. To illustrate this

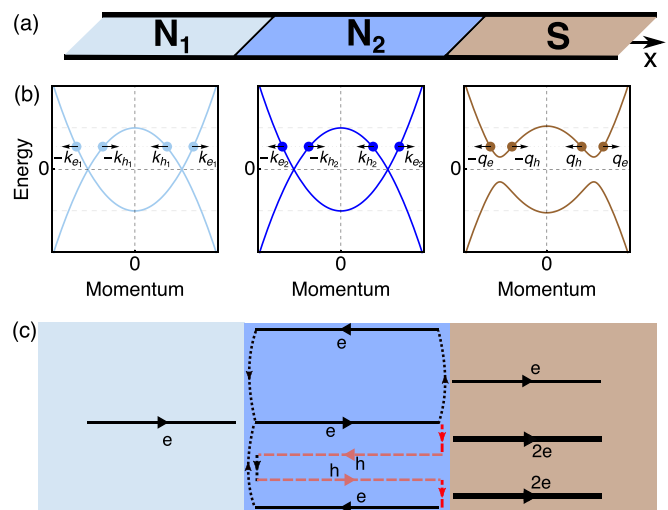


FIG. 1. (a) Sketch of a one-dimensional N_1N_2S junction. (b) Dispersion relation on each region at the same chemical potential. The arrows represent the velocity direction of electrons and holes with wave vectors $k_{e,h}$ in $N_{1,2}$ and $q_{e,h}$ in S. (c) Quasibound states in N_2 involving only normal reflections (top) or both normal and Andreev processes (bottom).

generic effect, we consider a normal metal–normal metal–superconductor (N_1N_2S) junction, as in Fig. 1(a), where confinement in the central region (N_2) enables the formation of qZESs. Interestingly, we find that these trivial qZESs produce ZBCPs, which might suggest some similarity to Majorana physics, although they exhibit a quantization of $4e^2/h$ and are less stable under variations of the chemical potential of the central region. Since most of the setups used to detect MBSs are prone to confinement, the emergence of topologically trivial qZESs, with quantized ZBCPs, can be a generic and ubiquitous effect in any superconducting hybrid system.

II. THEORETICAL FORMULATION

We consider a junction between a metallic and a superconducting contact separated by a ballistic one-dimensional region of length L , as shown in Fig. 1(a). This can be modeled by the Bogoliubov–de Gennes (BdG) Hamiltonian given by

$$H = \left[\frac{p^2}{2m} - \mu(x) \right] \tau_z + \Delta(x) \tau_x, \quad (1)$$

where $p = -i\hbar\partial_x$ is the momentum operator, m the electron effective mass, and $\mu(x) = \mu_{N_1}\Theta(-x-L) + \mu_{N_2}\Theta(x+L)\Theta(-x) + \mu_S\Theta(x)$ represents the chemical potential profile across the junction, with $\Theta(x)$ being the Heaviside step function and $\mu_{N_{1(2)}}$ and μ_S the chemical potentials in $N_{1(2)}$ and S regions, respectively. Moreover, $\Delta(x) = \Delta\Theta(x)$ represents the conventional spin-singlet s -wave pair potential with $\Delta \neq 0$ only in S. We contrast our findings with junctions where S is a topological superconductor, which we model substituting the pair potential in Eq. (1) by the equal-spin triplet p wave $\Delta(x) = \text{sgn}(p)\Delta\Theta(x)$ [75].

Diagonalizing the Hamiltonian in Eq. (1), we obtain the energy-momentum dispersion in each region presented in Fig. 1(b), with wave vectors in the N regions given by $k_{e_i, h_i} = k_{N_i} \sqrt{1 \pm \omega/\mu_{N_i}}$, with $k_{N_i} = \sqrt{2m\mu_{N_i}/\hbar^2}$ and $i = 1, 2$. In the S region, we obtain $q_{e, h} = k_S \sqrt{1 \pm \sqrt{\omega^2 - \Delta^2}/\mu_S}$, with $k_S = \sqrt{2m\mu_S/\hbar^2}$. These wave vectors characterize the right- and left-moving electrons and holes (electronlike and holelike quasiparticles) in the normal (superconducting) regions, indicated by filled circles with horizontal arrows in Fig. 1(b). Next, we use the scattering states associated to these quasiparticles to show how confinement in the middle region enables the formation of qZESs.

III. CONFINEMENT IN NORMAL-STATE JUNCTIONS

To understand the origin and impact of confinement in hybrid junctions modeled by Eq. (1), we first inspect the role of the intermediate N_2 region on transport across the junction when S is in its normal state (i.e., $\Delta = 0$). For this purpose, we calculate the conductance per spin channel across the NN_2N junction by matching the scattering states at the system interfaces, obtaining

$$T_N = \frac{2e^2/h}{1 + \left[\frac{k_e}{2k_{e_2}} + \frac{k_{e_2}}{2k_e} \right]^2 - \left[\frac{k_e}{2k_{e_2}} - \frac{k_{e_2}}{2k_e} \right]^2 \cos(2k_{e_2}L)}. \quad (2)$$

Note that Eq. (2) is defined for a single spin channel, so the conductance of a spinful NN_2N junction is $2T_N$. Without loss of generality, we assumed that the outer regions have the same chemical potential μ (i.e., $k_{e1} = q_e \equiv k_e$), while N_2 has μ_{N_2} and length L , thus producing a wave-vector mismatch between the middle and outer regions. For a detailed derivation of Eq. (2), see Supplemental Material [76]. The normal conductance T_N , Eq. (2), describes the possibility of an incident electron to be transmitted through the junction after experiencing several normal reflections inside the middle N_2 region. The effect of N_2 is captured in the cosine term in the denominator of Eq. (2), which signals the appearance of confinement and enables the formation of discrete energy levels whose number depends on the length of N_2 , similarly to a Fabry-Perot cavity. Consequently, there is a resonant transmission $T_N/(e^2/h) = 1$ either in the absence of N_2 , i.e., for $L = 0$ which leads to $\cos(2k_{e_2}L) = 1$, or when the wave vectors of the three regions are the same, $k_e = k_{e_2}$ [see Fig. 1(b)]. For a finite length N_2 region, with a chemical potential different than the outer regions, the resonant condition is $k_{e_2}L = n\pi$, with n and integer.

To visualize this behavior, we plot T_N in Fig. 2(a) as a function of the chemical potential μ_{N_2} . This allows us to identify the conditions for transport *on* and *off* resonance when the conductance is either maximum [$T_N/(e^2/h) = 1$] or minimum. *On resonance*, we obtain a ZBCP with periodicity determined by the length L [cf. Eq. (2)]. Interestingly, T_N can be resonant at exactly zero energy ($\omega = 0$), that is, solely as a result of confinement from the middle region due to the finite length and different chemical potential [see bottom panel of Fig. 2(a)]. As we show next, this rather general result is behind the formation of trivial Andreev qZESs, making this effect ubiquitous in superconducting heterostructures [77].

IV. CONFINEMENT IN SUPERCONDUCTING JUNCTIONS

We now analyze the consequences of confinement in transport across trivial and topological N_1N_2S junctions. In addition to normal reflections at both interfaces, Andreev reflections also take place at the N_2S interface, where incident electrons from N_2 are reflected back as holes [78]. Owing to these Andreev reflections the discrete energy levels of the middle region, discussed in the previous section, become coherent superpositions of electrons and holes. As a result, Andreev quasibound states are formed with properties that depend on the system parameters, as schematically shown by the bottom process of Fig. 1(c). This occurs for both trivial and topological junctions. To analyze the impact of this phenomenon on transport properties, we inspect the normalized conductance [79]

$$\sigma(\omega) = g \frac{e^2}{h} (1 - |r_{ee}(\omega)|^2 + |r_{eh}(\omega)|^2), \quad (3)$$

with $g = 2$ ($g = 1$) being the spin degeneracy factor for a trivial (topological) junction, and where r_{ee} and r_{eh} represent the normal and Andreev reflection amplitudes, respectively. These amplitudes are obtained by matching the scattering states of Eq. (1) at the interfaces of the N_1N_2S junction [76]. Equation (3) characterizes transport in both trivial and topological junctions, and we now discuss how it is affected by confinement effects.

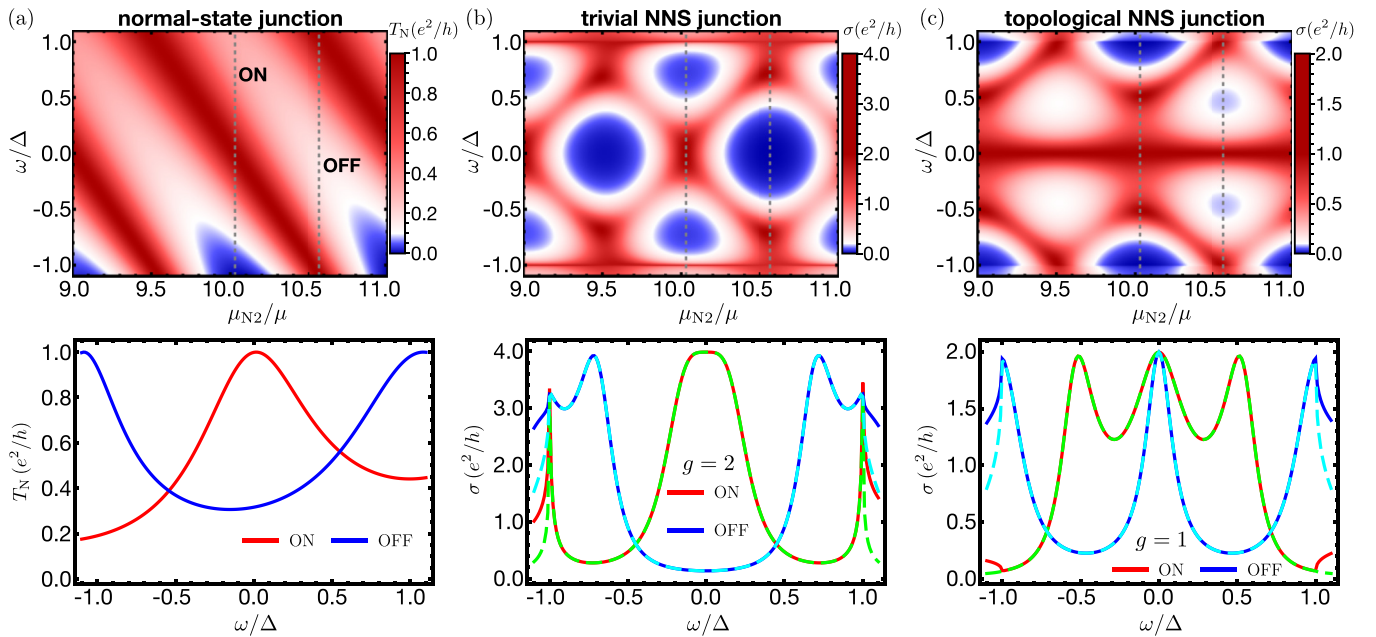


FIG. 2. Conductance as a function of energy and chemical potential of the intermediate region N_2 (top), or of the energy for on and off resonance (bottom), for (a) a normal state, (b) a trivial, or (c) a topological junction. The on- and off-resonance values of μ_{N_2} are plotted as dashed gray lines in the maps, labeled ON and OFF, respectively. For the bottom panels of (b) and (c) we plot $2|r_{eh}|^2$ using green (cyan) dashed lines for on (off) resonance. In all cases, $k_F L = 3\pi/2$, $\mu_{N_1} = \mu_S \equiv \mu = 2\Delta$.

We map the conductance σ as a function of the energy ω and the chemical potential of the middle region μ_{N_2} for a trivial ($g = 2$) and a topological ($g = 1$) $N_1 N_2 S$ junction in, respectively, Fig. 2(b) and Fig. 2(c). For both cases, the conductance develops resonances in a periodic fashion with maximum values (dark-red areas) that double those obtained when S is in its normal state [see Fig. 2(a)]. The ZBCPs are thus the combined result of a resonant tunneling effect through the effective quantum well caused by the central region N_2 and the doubling of the conductance at perfect transmission due to dominant Andreev scattering [79,80]. Here, the most important feature is that the conductance for a trivial $N_1 N_2 S$ junction exhibits a ZBCP for exactly the same parameters that result in a resonant normal-state transmission (see Fig. 2). Note that the appearance of this ZBCP can be tuned by the chemical potential of the middle region μ_{N_2} and remains robust under variations of other system parameters. Similar results can be obtained in a setup with electrostatic barriers separating the central and outer regions [81–86]. We have thus verified that these finite barriers do not affect the robustness of the ZBCP shown in Fig. 2(b). Moreover, the qZESs, and associated ZBCP, we report here can emerge also when $\mu_{N_1} \neq \mu_S$, which makes them more robust against asymmetry than similar resonances predicted by simpler models featuring single-level resonances [80]. In our setup, the presence or absence of a ZBCP directly corresponds to the on- or off-resonance regimes of the normal-state conductance, marked by vertical dotted lines in the maps of Fig. 2. This periodic appearance of the ZBCPs makes them very likely to occur in trivial junctions. By contrast, the ZBCP in topological junctions remains robust for any value of μ_{N_2} [see Fig. 2(c)]. To help distinguish the topological MBS from the trivial qZES one could test the stability of the ZBCP, e.g., by

varying the voltage gates or applying an external magnetic field.

On resonance, the ZBCP for a trivial junction is quantized as twice the normal-state conductance, i.e., $4T_N$ [compare Figs. 2(a) and 2(b)]. Such quantization disappears if μ_{N_2} is tuned out of resonance. The ZBCP is mainly due to Andreev processes fulfilling $\sigma(|\omega| < \Delta)/(2e^2/h) = 2|r_{eh}|^2$, with $|r_{eh}(\omega = 0)|^2 \rightarrow 1$ [see green and cyan dashed lines in Fig. 2(b)]. By contrast, the topological superconductor features a ZBCP both on and off resonance, with a perfect zero-energy Andreev reflection $|r_{eh}(\omega = 0)|^2 = 1$. The height of the ZBCP for topological junctions is, however, $2e^2/h$, and thus distinct to the ZBCP due to the qZESs reported here; an aspect that could also be useful when distinguishing the topological nature of both ZBCPs [see bottom panels in Figs. 2(b) and 2(c)]. It is also important to point out that the Andreev reflection in both trivial and topological junctions exhibit some important similarities. While topological junctions exhibit robust unitarity of Andreev reflection, confinement in trivial junctions can only approximately accommodate regimes of unitarity. These two situations are, however, difficult to distinguish by the naked eye.

The findings discussed above thus show that, on resonance, the ZBCPs for both trivial and topological junctions feature a very similar behavior. We stress again that this ZBCP for trivial junctions arises solely due to confinement effects of the central region. Importantly, our system does not include any spin-orbit coupling or magnetic field, in contrast to previous works [32–54], implying that the ZBCPs we find are not related to Majorana physics or topology. These results are thus in line with recent developments reporting that ZBCPs cannot be taken as a definitive indicator of topological superconductivity [50–52].

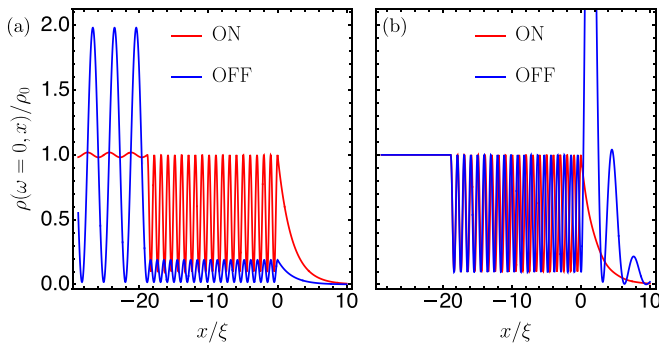


FIG. 3. Spatial dependence of the zero-energy LDOS for trivial (a) and topological (b) junctions, with the same parameters as Fig. 2, and red (blue) lines corresponding to on (off) resonance.

V. REAL SPACE ZERO-ENERGY LDOS

To better understand the behavior of the trivial qZES, we now study the spatial dependence of the local density of states (LDOS) ρ at zero energy. The LDOS is obtained from the retarded Green's function $G^r(x, x', \omega)$ associated to the BdG Hamiltonian in Eq. (1). To find $G^r(x, x', \omega)$ we follow a scattering Green's function approach [76] commonly used for superconducting junctions [87–94]. The Green's function $G^r(x, x', \omega)$ is a 2×2 matrix in Nambu (particle-hole) space, and the LDOS is then obtained as $\rho(\omega, x) = -\text{ImTr}[G^r(x, x, \omega)]/\pi$. The LDOS in S and N_2 exhibits a complex behavior, but in N_1 it is simply given by

$$\rho(\omega, x) = \frac{m}{\pi \hbar^2} \text{Im} \left\{ \sum_{\alpha=e,h} \frac{i}{k_\alpha} (1 + r_{\alpha\alpha} e^{-2is_\alpha k_\alpha x}) \right\}, \quad (4)$$

where $s_{e,h} = \pm 1$ and $r_{\alpha\alpha}$ represent normal reflection amplitudes. Deep inside the leftmost normal region, the LDOS adopts the simple form $\rho_0 = m(k_{e1}^{-1} + k_{h1}^{-1})/(\pi \hbar^2)$, which we use for normalization.

Because our interest is on the qZES, we present in Fig. 3 the spatial dependence of the zero-energy LDOS for trivial (a) and topological (b) junctions, when the chemical potential of the middle region μ_{N_2} is set on and off resonance (red and blue lines, respectively). For topological junctions, Fig. 3(b), the zero-energy LDOS is almost independent of the chemical potential in N_2 , μ_{N_2} . The zero-energy LDOS is perfectly flat on N_1 and oscillates with constant amplitude in N_2 , unaffected by variations of μ_{N_2} . Both features are a result of the perfect Andreev reflection taking place at the N_2 -S interface for $\omega = 0$, where the MBS is located, which, in turn, also promotes a perfect transmission at N - N_2 . As a result, $r_{ee} = 0$ in Eq. (4) and the zero-energy LDOS in N takes exactly the value of the bulk density ρ_0 . Hence, the robust profile of the zero-energy LDOS in topological junctions can be attributed to the presence of a MBS.

For trivial junctions on resonance, the magnitude and oscillations of the zero-energy LDOS [red curve in Fig. 3(a)] are very similar to those of topological junctions, albeit there are no MBSs present in this case. This indicates the formation of an extended qZES in N_2 , which is responsible for the finite LDOS at zero energy at the N - N_2 interface and causes the ZBCP in the conductance on resonance (Fig. 2). However,

off resonance, the zero-energy LDOS oscillations become vanishingly small, as seen in the blue curve of Fig. 3(a). Moreover, the zero-energy LDOS displays clear oscillations in the leftmost normal region N_1 , originating from the term proportional to $r_{\alpha\alpha}$ in Eq. (4). While the oscillations in N_1 are present both on and off resonance, their amplitude is greatly suppressed on resonance because normal reflections are finite but vanishingly small, i.e., $|r_{ee}|^2 \rightarrow 0$.

By the exposed above, the zero-energy LDOS on resonance for a trivial junction has the same qualitative behavior as that of a topological junction. While for trivial junctions on resonance the unitarity of the Andreev reflection is only approximately true, i.e., $|r_{eh}|^2 \rightarrow 1$, the presence of a MBS in topological junctions promotes a perfect Andreev reflection $|r_{eh}|^2 = 1$. However, whether the Andreev reflection unitarity is approximated or exact is rather challenging to distinguish in measurements, thus posing a critical question when interpreting ZBCPs. Consequently, discerning between the perfect Andreev reflection ($|r_{eh}|^2 = 1$) for a MBS and the approximate one ($|r_{eh}|^2 \lesssim 1$) for a trivial qZES on resonance would require a very sensitive scanning tunneling experiment.

VI. FINITE-SIZE EFFECTS

To showcase the emergence of confinement-induced qZESs, we have thus far considered a perfectly one-dimensional ballistic junction with semi-infinite outer leads. We now explore possible deviations from having finite-size outer leads or quasi-one-dimensional junctions. First, we performed tight-binding simulations on finite length systems, after discretizing Eq. (1) on a lattice, and verified that the main findings remain robust under more realistic conditions (see Ref. [76] for more details). Previously, the appearance of trivial qZESs has been confirmed in junctions with spin-orbit coupling and magnetism [34,72]. These junctions require that the middle region is within the helical regime, which, in some cases, can be a sufficient condition for the formation of qZESs [32]. Our work suggests that, in addition to other mechanisms showing the appearance of qZESs [32–54], confinement also deserves attention when analyzing ZBCPs in hybrid junctions.

Another finite-size effect is related to the finite cross section of semiconducting junctions [95,96]. Indeed, the Majorana condition in these setups is only fulfilled by a few transverse modes [97]. Even though a perfect one-dimensional regime is challenging to achieve, most Majorana platforms attempt to approach a one-dimensional limit by reducing the number of transverse modes contributing to transport. To study the impact of extra transport modes on the trivial ZBCP, we extend Eq. (1) to describe a two-dimensional system and denote as k_y the wave-vector component parallel to the interfaces [76]. The transport observables in Eqs. (2) and (3) must then be averaged over all incident modes, and the resonant condition for the confined states in N_2 becomes more complicated, as it now depends on the transverse wave vector k_y . Consequently, as we add extra modes, the magnitude of the ZBCP for trivial junctions on resonance is reduced, although the peak never disappears. Even though a quantization of the ZBCP in planar junctions is no longer possible, a conductance approaching the quantized value is still achievable in quasi-one-dimensional trivial junctions (see Ref. [76]).

VII. CONCLUSIONS

We have shown that quasi-zero-energy Andreev states can naturally emerge due to confinement effects in hybrid junctions based on conventional s -wave superconductors in the absence of any magnetic order. Such confinement-induced states, emerging here from a depleted or gated finite-length intermediate region, produce zero-bias conductance peaks and an enhanced zero-energy local density of states. These properties might suggest some similarity to Majorana physics. However, the trivial zero-bias peaks presented here have a different quantization ($4e^2/h$ instead of $2e^2/h$ for MBSs) and are less stable under variations of the chemical potential of the confined region. Note that confinement is a very common effect in hybrid junctions, including most Majorana nanowire experiments. Our results thus exemplify how ubiquitous trivial

zero-bias peaks can be in hybrid junctions, even without spin fields.

ACKNOWLEDGMENTS

We thank A. M. Black-Schaffer, T. M. Klapwijk, and A. Levy Yeyati for insightful discussions. J.C. acknowledges support from C.F. Liljewalchs stipendiestiftelse Foundation, the Knut and Alice Wallenberg Foundation through the Wallenberg Academy Fellows program, and the EU-COST Action CA-16218 NanocoHybri. P.B. acknowledges support from the Spanish CM “Talento Program” Project No. 2019-T1/IND-14088 and the Spanish Ministerio de Ciencia e Innovación Grant No. PID2020-117992GA-I00.

-
- [1] M. Sato and S. Fujimoto, Majorana fermions and topology in superconductors, *J. Phys. Soc. Jpn.* **85**, 072001 (2016).
- [2] M. Sato and Y. Ando, Topological superconductors: A review, *Rep. Prog. Phys.* **80**, 076501 (2017).
- [3] R. Aguado, Majorana quasiparticles in condensed matter, *Riv. Nuovo Cimento* **40**, 523 (2017).
- [4] R. M. Lutchyn, E. P. Bakkers, L. P. Kouwenhoven, P. Krogstrup, C. M. Marcus, and Y. Oreg, Majorana zero modes in superconductor–semiconductor heterostructures, *Nat. Rev. Mater.* **3**, 52 (2018).
- [5] H. Zhang, D. E. Liu, M. Wimmer, and L. P. Kouwenhoven, Next steps of quantum transport in Majorana nanowire devices, *Nat. Commun.* **10**, 5128 (2019).
- [6] C. W. J. Beenakker, Search for non-Abelian Majorana braiding statistics in superconductors, *SciPost Phys. Lect. Notes* **15** (2020).
- [7] Y. Oreg and F. von Oppen, Majorana zero modes in networks of Cooper-pair boxes: Topologically ordered states and topological quantum computation, *Annu. Rev. Condens. Matter Phys.* **11**, 397 (2020).
- [8] R. Aguado, A perspective on semiconductor-based superconducting qubits, *Appl. Phys. Lett.* **117**, 240501 (2020).
- [9] R. M. Lutchyn, J. D. Sau, and S. Das Sarma, Majorana Fermions and a Topological Phase Transition in Semiconductor-Superconductor Heterostructures, *Phys. Rev. Lett.* **105**, 077001 (2010).
- [10] Y. Oreg, G. Refael, and F. von Oppen, Helical Liquids and Majorana Bound States in Quantum Wires, *Phys. Rev. Lett.* **105**, 177002 (2010).
- [11] A. Y. Kitaev, Unpaired Majorana fermions in quantum wires, *Phys. Usp.* **44**, 131 (2001).
- [12] D. A. Ivanov, Non-Abelian Statistics of Half-Quantum Vortices in p -Wave Superconductors, *Phys. Rev. Lett.* **86**, 268 (2001).
- [13] C. Nayak, S. H. Simon, A. Stern, M. Freedman, and S. Das Sarma, Non-Abelian anyons and topological quantum computation, *Rev. Mod. Phys.* **80**, 1083 (2008).
- [14] S. D. Sarma, M. Freedman, and C. Nayak, Majorana zero modes and topological quantum computation, *npj Quantum Inf.* **1**, 15001 (2015).
- [15] J. Alicea, Y. Oreg, G. Refael, F. Von Oppen, and M. P. Fisher, Non-Abelian statistics and topological quantum information processing in 1D wire networks, *Nat. Phys.* **7**, 412 (2011).
- [16] D. Aasen, M. Hell, R. V. Mishmash, A. Higginbotham, J. Danon, M. Leijnse, T. S. Jespersen, J. A. Folk, C. M. Marcus, K. Flensberg, and J. Alicea, Milestones Toward Majorana-Based Quantum Computing, *Phys. Rev. X* **6**, 031016 (2016).
- [17] Y. Tanaka and S. Kashiwaya, Theory of Tunneling Spectroscopy of d -Wave Superconductors, *Phys. Rev. Lett.* **74**, 3451 (1995).
- [18] C. J. Bolech and E. Demler, Observing Majorana Bound States in p -Wave Superconductors Using Noise Measurements in Tunneling Experiments, *Phys. Rev. Lett.* **98**, 237002 (2007).
- [19] K. T. Law, P. A. Lee, and T. K. Ng, Majorana Fermion Induced Resonant Andreev Reflection, *Phys. Rev. Lett.* **103**, 237001 (2009).
- [20] K. Flensberg, Tunneling characteristics of a chain of Majorana bound states, *Phys. Rev. B* **82**, 180516(R) (2010).
- [21] B. Lu, P. Burset, Y. Tanuma, A. A. Golubov, Y. Asano, and Y. Tanaka, Influence of the impurity scattering on charge transport in unconventional superconductor junctions, *Phys. Rev. B* **94**, 014504 (2016).
- [22] P. Burset, B. Lu, S. Tamura, and Y. Tanaka, Current fluctuations in unconventional superconductor junctions with impurity scattering, *Phys. Rev. B* **95**, 224502 (2017).
- [23] V. Mourik, K. Zuo, S. Frolov, S. Plissard, E. Bakkers, and L. Kouwenhoven, Signatures of Majorana fermions in hybrid superconductor-semiconductor nanowire devices, *Science* **336**, 1003 (2012).
- [24] A. P. Higginbotham, S. M. Albrecht, G. Kirsanskas, W. Chang, F. Kuemmeth, P. Krogstrup, T. S. J. J. Nygård, K. Flensberg, and C. M. Marcus, Parity lifetime of bound states in a proximitized semiconductor nanowire, *Nat. Phys.* **11**, 1017 (2015).
- [25] M. T. Deng, S. Vaitiekėnas, E. B. Hansen, J. Danon, M. Leijnse, K. Flensberg, J. Nygård, P. Krogstrup, and C. M. Marcus, Majorana bound state in a coupled quantum-dot hybrid-nanowire system, *Science* **354**, 1557 (2016).
- [26] S. M. Albrecht, A. P. Higginbotham, M. Madsen, F. Kuemmeth, T. S. Jespersen, J. Nygård, P. Krogstrup, and C. M. Marcus, Exponential protection of zero modes in Majorana islands, *Nature (London)* **531**, 206 (2016).
- [27] H. Zhang, Önder Gül, S. Conesa-Boj, K. Zuo, V. Mourik, F. K. de Vries, J. van Veen, D. J. van Woerkom, M. P. Nowak, M. Wimmer *et al.*, Ballistic superconductivity in semiconductor nanowires, *Nat. Commun.* **8**, 16025 (2017).

- [28] H. J. Suominen, M. Kjaergaard, A. R. Hamilton, J. Shabani, C. J. Palmstrøm, C. M. Marcus, and F. Nichele, Zero-Energy Modes from Coalescing Andreev States in a Two-Dimensional Semiconductor-Superconductor Hybrid Platform, *Phys. Rev. Lett.* **119**, 176805 (2017).
- [29] F. Nichele, A. C. C. Drachmann, A. M. Whiticar, E. C. T. O'Farrell, H. J. Suominen, A. Fornieri, T. Wang, G. C. Gardner, C. Thomas, A. T. Hatke *et al.*, Scaling of Majorana Zero-Bias Conductance Peaks, *Phys. Rev. Lett.* **119**, 136803 (2017).
- [30] Hao Zhang, Michiel W. A. de Moor, Jouri D. S. Bommer, Di Xu, Guanzhong Wang, Nick van Loo, Chun-Xiao Liu, Sasa Gazibegovic, John A. Logan, Diana Car *et al.*, Large zero-bias peaks in InSb-Al hybrid semiconductor-superconductor nanowire devices, [arXiv:2101.11456](https://arxiv.org/abs/2101.11456).
- [31] Ö. Gül, H. Zhang, J. D. Bommer, M. W. de Moor, D. Car, S. R. Plissard, E. P. Bakkers, A. Geresdi, K. Watanabe, T. Taniguchi *et al.*, Ballistic Majorana nanowire devices, *Nat. Nanotechnol.* **13**, 192 (2018).
- [32] G. Kells, D. Meidan, and P. W. Brouwer, Near-zero-energy end states in topologically trivial spin-orbit coupled superconducting nanowires with a smooth confinement, *Phys. Rev. B* **86**, 100503(R) (2012).
- [33] E. Prada, P. San-Jose, and R. Aguado, Transport spectroscopy of *NS* nanowire junctions with Majorana fermions, *Phys. Rev. B* **86**, 180503(R) (2012).
- [34] J. Cayao, E. Prada, P. San-Jose, and R. Aguado, SNS junctions in nanowires with spin-orbit coupling: Role of confinement and helicity on the subgap spectrum, *Phys. Rev. B* **91**, 024514 (2015).
- [35] P. San-José, J. Cayao, E. Prada, and R. Aguado, Majorana bound states from exceptional points in non-topological superconductors, *Sci. Rep.* **6**, 21427 (2016).
- [36] C.-X. Liu, J. D. Sau, T. D. Stanescu, and S. Das Sarma, Andreev bound states versus Majorana bound states in quantum dot-nanowire-superconductor hybrid structures: Trivial versus topological zero-bias conductance peaks, *Phys. Rev. B* **96**, 075161 (2017).
- [37] A. Ptok, A. Kobiałka, and T. Domański, Controlling the bound states in a quantum-dot hybrid nanowire, *Phys. Rev. B* **96**, 195430 (2017).
- [38] C. Fleckenstein, F. Domínguez, N. Traverso Ziani, and B. Trauzettel, Decaying spectral oscillations in a Majorana wire with finite coherence length, *Phys. Rev. B* **97**, 155425 (2018).
- [39] C. Reeg, O. Dmytruk, D. Chevallier, D. Loss, and J. Klinovaja, Zero-energy Andreev bound states from quantum dots in proximitized Rashba nanowires, *Phys. Rev. B* **98**, 245407 (2018).
- [40] S. Pal and C. Benjamin, Yu-Shiba-Rusinov bound states induced by a spin flipper in the vicinity of a s-wave superconductor, *Sci. Rep.* **8**, 11949 (2018).
- [41] J. Chen, B. D. Woods, P. Yu, M. Hocevar, D. Car, S. R. Plissard, E. P. A. M. Bakkers, T. D. Stanescu, and S. M. Frolov, Ubiquitous Non-Majorana Zero-Bias Conductance Peaks in Nanowire Devices, *Phys. Rev. Lett.* **123**, 107703 (2019).
- [42] T. D. Stanescu and S. Tewari, Robust low-energy Andreev bound states in semiconductor-superconductor structures: Importance of partial separation of component Majorana bound states, *Phys. Rev. B* **100**, 155429 (2019).
- [43] T. Dvir, M. Aprili, C. H. L. Quay, and H. Steinberg, Zeeman Tunability of Andreev Bound States in Van Der Waals Tunnel Barriers, *Phys. Rev. Lett.* **123**, 217003 (2019).
- [44] A. Vuik, B. Nijholt, A. R. Akhmerov, and M. Wimmer, Reproducing topological properties with quasi-Majorana states, *SciPost Phys.* **7**, 61 (2019).
- [45] J. Avila, F. Peñaranda, E. Prada, P. San-Jose, and R. Aguado, Non-Hermitian topology as a unifying framework for the Andreev versus Majorana states controversy, *Commun. Phys.* **2**, 133 (2019).
- [46] H. Pan and S. Das Sarma, Physical mechanisms for zero-bias conductance peaks in Majorana nanowires, *Phys. Rev. Research* **2**, 013377 (2020).
- [47] C. Jünger, R. Delagrangé, D. Chevallier, S. Lehmann, K. A. Dick, C. Thelander, J. Klinovaja, D. Loss, A. Baumgartner, and C. Schönenberger, Magnetic-Field-Independent Subgap States in Hybrid Rashba Nanowires, *Phys. Rev. Lett.* **125**, 017701 (2020).
- [48] D. Razmadze, E. C. T. O'Farrell, P. Krogstrup, and C. M. Marcus, Quantum Dot Parity Effects in Trivial and Topological Josephson Junctions, *Phys. Rev. Lett.* **125**, 116803 (2020).
- [49] O. Dmytruk, D. Loss, and J. Klinovaja, Pinning of Andreev bound states to zero energy in two-dimensional superconductor-semiconductor Rashba heterostructures, *Phys. Rev. B* **102**, 245431 (2020).
- [50] P. Yu, J. Chen, M. Gomanko, G. Badawy, E. P. A. M. Bakkers, K. Zuo, V. Mourik, and S. M. Frolov, Non-Majorana states yield nearly quantized conductance in proximitized nanowires, *Nat. Phys.* **17**, 482 (2021).
- [51] M. Valentini, F. Peñaranda, A. Hofmann, M. Brauns, R. Hauschild, P. Krogstrup, P. San-Jose, E. Prada, R. Aguado, and G. Katsaros, Nontopological zero-bias peaks in full-shell nanowires induced by flux-tunable Andreev states, *Science* **373**, 82 (2021).
- [52] E. Prada, P. San-Jose, M. W. de Moor, A. Geresdi, E. J. Lee, J. Klinovaja, D. Loss, J. Nygård, R. Aguado, and L. P. Kouwenhoven, From Andreev to Majorana bound states in hybrid superconductor-semiconductor nanowires, *Nat. Rev. Phys.* **2**, 575 (2020).
- [53] N. T. Ziani, C. Fleckenstein, L. Vigliotti, B. Trauzettel, and M. Sassetti, From fractional solitons to Majorana fermions in a paradigmatic model of topological superconductivity, *Phys. Rev. B* **101**, 195303 (2020).
- [54] C. Moore, C. Zeng, T. D. Stanescu, and S. Tewari, Quantized zero-bias conductance plateau in semiconductor-superconductor heterostructures without topological Majorana zero modes, *Phys. Rev. B* **98**, 155314 (2018).
- [55] C. Moore, T. D. Stanescu, and S. Tewari, Two-terminal charge tunneling: Disentangling Majorana zero modes from partially separated Andreev bound states in semiconductor-superconductor heterostructures, *Phys. Rev. B* **97**, 165302 (2018).
- [56] C.-X. Liu, J. D. Sau, and S. Das Sarma, Distinguishing topological Majorana bound states from trivial Andreev bound states: Proposed tests through differential tunneling conductance spectroscopy, *Phys. Rev. B* **97**, 214502 (2018).
- [57] M. Hell, K. Flensberg, and M. Leijnse, Distinguishing Majorana bound states from localized Andreev bound states by interferometry, *Phys. Rev. B* **97**, 161401(R) (2018).
- [58] L. S. Ricco, M. de Souza, M. S. Figueira, I. A. Shelykh, and A. C. Seridonio, Spin-dependent zero-bias peak in a hybrid nanowire-quantum dot system: Distinguishing isolated

- Majorana fermions from Andreev bound states, *Phys. Rev. B* **99**, 155159 (2019).
- [59] K. Yavilberg, E. Ginossar, and E. Grosfeld, Differentiating Majorana from Andreev bound states in a superconducting circuit, *Phys. Rev. B* **100**, 241408(R) (2019).
- [60] O. A. Awoga, J. Cayao, and A. M. Black-Schaffer, Supercurrent Detection of Topologically Trivial Zero-Energy States in Nanowire Junctions, *Phys. Rev. Lett.* **123**, 117001 (2019).
- [61] J. Schulenburg and K. Flensberg, Absence of supercurrent sign reversal in a topological junction with a quantum dot, *Phys. Rev. B* **101**, 014512 (2020).
- [62] G. Zhang and C. Spånslätt, Distinguishing between topological and quasi Majorana zero modes with a dissipative resonant level, *Phys. Rev. B* **102**, 045111 (2020).
- [63] O. Kashuba, B. Sothmann, P. Buset, and B. Trauzettel, Majorana STM as a perfect detector of odd-frequency superconductivity, *Phys. Rev. B* **95**, 174516 (2017).
- [64] A. Schuray, M. Rammner, and P. Recher, Signatures of the Majorana spin in electrical transport through a Majorana nanowire, *Phys. Rev. B* **102**, 045303 (2020).
- [65] A. Grabsch, Y. Cheipesh, and C. W. J. Beenakker, Dynamical signatures of ground-state degeneracy to discriminate against Andreev levels in a Majorana fusion experiment, *Adv. Quantum Technol.* **3**, 1900110 (2020).
- [66] H. Pan, J. D. Sau, and S. Das Sarma, Three-terminal non-local conductance in Majorana nanowires: Distinguishing topological and trivial in realistic systems with disorder and inhomogeneous potential, *Phys. Rev. B* **103**, 014513 (2021).
- [67] D. Liu, Z. Cao, X. Liu, H. Zhang, and D. E. Liu, Topological Kondo device for distinguishing quasi-Majorana and Majorana signatures, [arXiv:2009.09996](https://arxiv.org/abs/2009.09996).
- [68] J. Danon, A. B. Hellenes, E. B. Hansen, L. Casparis, A. P. Higginbotham, and K. Flensberg, Nonlocal Conductance Spectroscopy of Andreev Bound States: Symmetry Relations and BCS Charges, *Phys. Rev. Lett.* **124**, 036801 (2020).
- [69] L. S. Ricco, J. E. Sanches, Y. Marques, M. de Souza, M. S. Figueira, I. A. Shelykh, and A. C. Seridonio, Topological iso-conductance signatures in Majorana nanowires, *Sci. Rep.* **11**, 17310 (2021).
- [70] M. Thamm and B. Rosenow, Transmission amplitude through a Coulomb blockaded Majorana wire, *Phys. Rev. Research* **3**, 023221 (2021).
- [71] W. Chen, J. Wang, Y. Wu, J. Liu, and X. C. Xie, Non-Abelian statistics of Majorana zero modes in the presence of an Andreev bound state, [arXiv:2005.00735](https://arxiv.org/abs/2005.00735).
- [72] J. Cayao and A. M. Black-Schaffer, Distinguishing trivial and topological zero energy states in long nanowire junctions, *Phys. Rev. B* **104**, L020501 (2021).
- [73] C. Fleckenstein, N. T. Ziani, A. Calzona, M. Sasseti, and B. Trauzettel, Formation and detection of Majorana modes in quantum spin Hall trenches, *Phys. Rev. B* **103**, 125303 (2021).
- [74] L. S. Ricco, V. K. Kozin, A. C. Seridonio, and I. A. Shelykh, Accessing the degree of Majorana nonlocality with photons, [arXiv:2105.05925](https://arxiv.org/abs/2105.05925).
- [75] A. Tsintzis, A. M. Black-Schaffer, and J. Cayao, Odd-frequency superconducting pairing in Kitaev-based junctions, *Phys. Rev. B* **100**, 115433 (2019).
- [76] See Supplemental Material at <http://link.aps.org/supplemental/10.1103/PhysRevB.104.134507>, including Refs. [3,11,80,87,89,96], for details on how we calculate the conductance, the Green's functions, and the LDOS for N_1N_2S junctions. We also present the numerical simulations for finite-size and quasi-one-dimensional systems.
- [77] T. M. Klapwijk and S. A. Ryabchun, Direct observation of ballistic Andreev reflection, *J. Exp. Theor. Phys.* **119**, 997 (2014).
- [78] T. M. Klapwijk, Proximity effect from an Andreev perspective, *J. Supercond.* **17**, 593 (2004).
- [79] G. E. Blonder, M. Tinkham, and T. M. Klapwijk, Transition from metallic to tunneling regimes in superconducting microconstrictions: Excess current, charge imbalance, and supercurrent conversion, *Phys. Rev. B* **25**, 4515 (1982).
- [80] C. W. J. Beenakker, Quantum transport in semiconductor-superconductor microjunctions, *Phys. Rev. B* **46**, 12841 (1992).
- [81] B. J. van Wees, P. de Vries, P. Magnée, and T. M. Klapwijk, Excess Conductance of Superconductor-Semiconductor Interfaces Due to Phase Conjugation Between Electrons and Holes, *Phys. Rev. Lett.* **69**, 510 (1992).
- [82] A. F. Volkov, A. V. Zaitsev, and T. M. Klapwijk, Proximity effect under nonequilibrium conditions in double-barrier superconducting junctions, *Phys. C (Amsterdam, Neth.)* **210**, 21 (1993).
- [83] J. A. Melsen and C. W. J. Beenakker, Reflectionless tunneling through a double-barrier NS junction, *Phys. B (Amsterdam, Neth.)* **203**, 219 (1994).
- [84] M. Schechter, Y. Imry, and Y. Levinson, Reflectionless tunneling in ballistic normal-metal-superconductor junctions, *Phys. Rev. B* **64**, 224513 (2001).
- [85] H. Takayanagi, E. Toyoda, and T. Akazaki, Reflectionless tunneling due to Andreev reflection in a gated superconductor-semiconductor junction, *Phys. C (Amsterdam, Neth.)* **367**, 204 (2002).
- [86] G. B. Lesovik and I. A. Sadovskyy, Scattering matrix approach to the description of quantum electron transport, *Phys. Usp.* **54**, 1007 (2011).
- [87] W. L. McMillan, Theory of Superconductor-Normal Metal Interfaces, *Phys. Rev.* **175**, 559 (1968).
- [88] A. Furusaki and M. Tsukada, DC Josephson effect and Andreev reflection, *Solid State Commun.* **78**, 299 (1991).
- [89] S. Kashiwaya and Y. Tanaka, Tunneling effects on surface bound states in unconventional superconductors, *Rep. Prog. Phys.* **63**, 1641 (2000).
- [90] W. J. Herrera, P. Buset, and A. Levy Yeyati, A Green function approach to graphene-superconductor junctions with well-defined edges, *J. Phys.: Condens. Matter* **22**, 275304 (2010).
- [91] P. Buset, B. Lu, G. Tkachov, Y. Tanaka, E. M. Hankiewicz, and B. Trauzettel, Superconducting proximity effect in three-dimensional topological insulators in the presence of a magnetic field, *Phys. Rev. B* **92**, 205424 (2015).
- [92] B. Lu, P. Buset, K. Yada, and Y. Tanaka, Tunneling spectroscopy and Josephson current of superconductor-ferromagnet hybrids on the surface of a 3D Ti, *Supercond. Sci. Technol.* **28**, 105001 (2015).
- [93] J. Cayao and A. M. Black-Schaffer, Odd-frequency superconducting pairing and subgap density of states at the edge of a two-dimensional topological insulator without magnetism, *Phys. Rev. B* **96**, 155426 (2017).
- [94] B. Lu and Y. Tanaka, Study on Green's function on topological insulator surface, *Philos. Trans. R. Soc. (London), Ser. A* **376**, 20150246 (2018).

- [95] J. Wiedenmann, E. Liebhaber, J. Kübert, E. Bocquillon, P. Buset, C. Ames, H. Buhmann, T. M. Klapwijk, and L. W. Molenkamp, Transport spectroscopy of induced superconductivity in the three-dimensional topological insulator HgTe, *Phys. Rev. B* **96**, 165302 (2017).
- [96] D. Breunig, S.-B. Zhang, B. Trauzettel, and T. M. Klapwijk, Directional electron filtering at a superconductor-semiconductor interface, *Phys. Rev. B* **103**, 165414 (2021).
- [97] J. S. Lim, L. Serra, R. López, and R. Aguado, Magnetic-field instability of Majorana modes in multiband semiconductor wires, *Phys. Rev. B* **86**, 121103(R) (2012).